Optimized Schwarz Waveform Relaxation for Porous Media Applications

Caroline Japhet[1] and Pascal Omnes[2]

[1] LAGA, Université Paris XIII, 99 Avenue J-B Clément, 93430 Villetaneuse, France and CSCAMM, University of Maryland College Park, MD 20742 USA, japhet@math.univ-paris13.fr, partially supported by GdR MoMaS.
[2] CEA, DEN, DM2S-SFME-LSET, F91191 Gif sur Yvette Cedex, France., pascal.omnes@cea.fr.

UNCORRECTED PROOF

1 Introduction

Far field simulations of underground nuclear waste disposal involve a number of challenges for numerical simulations: widely differing lengths and time-scales, highly variable coefficients and stringent accuracy requirements. In the site under consideration by the French Agency for Nuclear Waste Management (ANDRA), the repository would be located in a highly impermeable geological layer, whereas the layers just above and below have very different physical properties (see [1]). It is then natural to use different time steps in the various layers, so as to match the time step with the physics. To do this, we propose to adapt a global in time domain decomposition method, based on Schwarz waveform relaxation algorithms, to problems in heterogeneous media. This method has been introduced and analyzed for linear advection-reaction-diffusion problems with continuous coefficients [2, 6] and extended to discontinuous coefficients [3, 4], with asymptotically optimized Robin transmission conditions in [3]. The method is extended to higher dimension in [4] with convergence results and error estimates for rectangular or strip subdomains.

This method is extended to problems with discontinuous porosity in [5]. A new aproach is proposed to determine optimized transmission conditions for domains with highly variable lengths. In this paper we analyse this approach in 1d.

Our model problem for the radionuclide transport is the one dimensional advection-diffusion-reaction equation

$$\begin{aligned} \varphi\partial_t u + a\partial_x u - \partial_x(\nu\partial_x u) + bu = f, \quad &\text{on } \mathbb{R}\times(0,T), \\ u(0,x) = u_0(x), \quad &x\in\mathbb{R}. \end{aligned} \tag{1}$$

We focus on a model problem to show the effect of subdomains with widely differing sizes. We consider a decomposition in $\Omega_1 = (-\infty,0)$, $\Omega_2 = (0,L)$, $\Omega_3 = (L,\infty)$ with $L << 1$. The reaction coefficient b is taken constant and the coefficients a, ν, and φ are assumed constant on each Ω_k, but may be discontinuous at $x = 0$ and $x = L$,

R. Bank et al. (eds.), *Domain Decomposition Methods in Science and Engineering XX*, Lecture Notes in Computational Science and Engineering 91,
DOI 10.1007/978-3-642-35275-1__69, © Springer-Verlag Berlin Heidelberg 2013

$$\varphi = \varphi_k, \quad a = a_k, \quad \nu = \nu_k, \quad x \in \Omega_k.$$

We introduce the notations

$$\begin{aligned}&\mathscr{L}_k v := \varphi_k \partial_t v + a_k \partial_x v - \partial_x(\nu_k \partial_x v) + bv, \quad \text{on } \Omega_k \times (0,T),\\ &\boldsymbol{\varphi} := (\varphi_1, \varphi_2, \varphi_3), \boldsymbol{a} := (a_1, a_2, a_3), \boldsymbol{\nu} := (\nu_1, \nu_2, \nu_3).\end{aligned}$$

Problem (1) is equivalent to solving problems in subdomains Ω_k

$$\begin{aligned}\mathscr{L}_k u_k &= f, \quad \text{on } \Omega_k \times (0,T),\\ u_k(0,x) &= u_0(x), \quad x \in \Omega_k.\end{aligned}$$

with coupling conditions on the interface $\Gamma_{k,\ell}$ between two neighboring subdomains Ω_k and Ω_ℓ given by

$$u_k = u_\ell, \quad \big(\nu_k \partial_x - a_k\big)\, u_k = \big(\nu_\ell \partial_x - a_\ell\big)\, u_\ell, \quad \text{on } \Gamma_{k,\ell} \times (0,T). \tag{2}$$

2 Domain Decomposition Algorithm

A simple algorithm based on relaxation of the coupling conditions (2) does not converge in general (see [7]). Following previous works [2–4], we introduce the Schwarz waveform relaxation algorithm

$$\begin{aligned}\mathscr{L}_k u_k^n &= f, \quad \text{on } \Omega_k \times (0,T),\\ u_k^n(0,x) &= u_0(x), \quad x \in \Omega_k,\\ \big(\nu_k \partial_x - a_k\big)\, u_k^n + \mathscr{S}_{k,\ell} u_k^n &= \big(\nu_\ell \partial_x - a_\ell\big)\, u_\ell^{n-1} + \mathscr{S}_{k,\ell} u_\ell^{n-1}, \quad \text{on } \Gamma_{k,\ell} \times (0,T),\end{aligned} \tag{3}$$

where $\mathscr{S}_{k,\ell}$ are linear operators in time and space, defined by

$$\mathscr{S}_{k,\ell}\psi = \bar{p}_{k,\ell}\psi + \bar{q}_{k,\ell}\partial_t \psi.$$

The case $\bar{q}_{k,\ell} = 0$ corresponds to Robin transmission conditions, while the case $\bar{q}_{k,\ell} \neq 0$ corresponds to first order transmission conditions. The well-posedness and convergence have been analyzed for constant porosity in [3] and in higher dimension in [4]. The transmission conditions in (3) imply the coupling conditions (2) at convergence, and lead at the same time to an efficient algorithm, for suitable parameters $\bar{p}_{k,\ell}$ and $\bar{q}_{k,\ell}$ obtained from an optimization of the convergence factor.

Similarly, $\mathscr{S}_{k,\ell}$ are approximations of the best operators related to transparent boundary operators. They can be found using Fourier analysis in the two half-spaces case. This analysis has been done for discontinuous coefficients [3], and in higher dimension and continuous coefficients [2]. The min-max problem has been analysed in one dimension in [3] with asymptotical Robin parameters.

In the field of nuclear waste computations, domains of meter scale are embedded in domains of kilometer scale. The previous optimization of the convergence factor does not take into account the high variability of the domains lengths. Following [5], we determine optimized transmission conditions through the minimization of a convergence factor that takes into account this variability.

UNCORRECTED PROOF

2.1 Optimal Transmission Conditions

In order to determine the optimal transmission operators $\mathscr{S}_{k,\ell}$, we compute the convergence factor of the algorithm. Since the problem is linear, we consider the algorithm (3) on the error (i.e. with $f=0$ and $u_0=0$). In order to use a Fourier transform in time, we assume that all functions are extended by 0 for $t<0$.

Let $e_k^n = u_k^n - u$ be the error in Ω_k at iteration k. The operators $\mathscr{S}_{k,\ell}$ are related to their symbols $\sigma_{k,\ell}(\omega)$ by

$$\mathscr{S}_{k,\ell}u(t) = \frac{1}{2\pi}\int \sigma_{k,\ell}(\omega)\hat{u}(\omega)e^{i\omega t}\,d\omega.$$

The Fourier transforms $\hat{e}_k^n$ in time of e_k^n are solutions of the ordinary differential equation in the x variable

$$-\nu_k\partial_{xx}^2\hat{e} + a_k\partial_x\hat{e} + (i\varphi_k\omega + b)\hat{e} = 0.$$

The characteristic roots are

$$r^{\pm}(a_k,\nu_k,\varphi_k,b,\omega) = \frac{a_k \pm \sqrt{d_k}}{2\nu_k}, \quad d_k = a_k^2 + 4\nu_k(i\varphi_k\omega + b). \tag{4}$$

Since $\Re r^+ > 0$, $\Re r^- < 0$, and since we look for solutions which do not increase exponentially in $|x|$, we obtain

$$\begin{aligned} &\hat{e}_1^n(x,\omega) = \alpha_1^n(\omega)e^{r^+(a_1,\nu_1,\varphi_1,b,\omega)x}, \quad \hat{e}_3^n(x,\omega) = \alpha_3^n(\omega)e^{r^-(a_3,\nu_3,\varphi_3,b,\omega)x},\\ &\hat{e}_2^n(x,\omega) = \alpha_2^n(\omega)e^{r^+(a_2,\nu_2,\varphi_2,b,\omega)x} + \beta_2^n(\omega)e^{r^-(a_2,\nu_2,\varphi_2,b,\omega)x}. \end{aligned} \tag{5}$$

We set $\xi^n = (\alpha_1^n, \alpha_2^n, \beta_2^n, \alpha_3^n)^t$, and $r_k^{\pm} = r^{\pm}(a_k,\nu_k,\varphi_k,b,\omega)$. We define the variables $s_k = s_k(\omega,L)$, $1 \le k \le 8$, by

$$s_1 = \frac{\nu_2 r_2^- - \sigma_{1,2}}{\nu_1 r_1^- - \sigma_{1,2}}, \; s_2 = \frac{\nu_2 r_2^+ - \sigma_{1,2}}{\nu_1 r_1^- - \sigma_{1,2}}, \; s_3 = \frac{\nu_2 r_2^+ - \sigma_{2,3}}{\nu_2 r_2^- - \sigma_{2,3}} \cdot e^{(r_2^- - r_2^+)L},$$

$$s_5 = \frac{\nu_2 r_2^- + \sigma_{2,1}}{\nu_2 r_2^+ + \sigma_{2,1}}, \; s_7 = \frac{\nu_2 r_2^- + \sigma_{3,2}}{\nu_3 r_3^+ + \sigma_{3,2}} e^{(r_2^+ - r_3^-)L}, \; s_8 = \frac{\nu_2 r_2^+ + \sigma_{3,2}}{\nu_3 r_3^+ + \sigma_{3,2}} e^{(r_2^- - r_3^-)L},$$

$$s_4 = \frac{\nu_1 r_1^- + \sigma_{2,1}}{\nu_2 r_2^+ + \sigma_{2,1}} \cdot \frac{1}{D}, \; s_6 = \frac{\nu_3 r_3^+ - \sigma_{2,3}}{\nu_2 r_2^- - \sigma_{2,3}} \cdot \frac{e^{(r_3^- - r_2^+)L}}{D}, \text{ with } D = s_3 s_5 - 1.$$

We insert (5) into the transmission conditions in (3), and obtain for $n \ge 2$,

$$\xi^n = M\xi^{n-1},$$

where the matrix $M = M(\omega,L)$ is defined by

$$M = \begin{pmatrix} 0 & s_1 & s_2 & 0 \\ s_3 s_4 & 0 & 0 & -s_6 \\ -s_4 & 0 & 0 & s_5 s_6 \\ 0 & s_7 & s_8 & 0 \end{pmatrix}.$$

The convergence factor $\rho(\omega,L)$ for each $\omega \in \mathbb{R}$ is the spectral radius of M.

UNCORRECTED PROOF

Remark 1. The choice for the symbols $\sigma_{k,\ell}$

$$\sigma_{1,2} = \nu_2 r_2^+, \quad \sigma_{2,1} = -\nu_1 r_1^-, \quad \sigma_{2,3} = \nu_3 r_3^+, \quad \sigma_{3,2} = -\nu_2 r_2^-, \tag{6}$$

leads to $M^2 = 0$ and thus to optimal convergence in three iterations.

Proposition 1. *The convergence factor is given by*

$$\rho(\omega, L) = \sqrt{\max(|\lambda^-|, |\lambda^+|)},$$

where $\lambda^\pm = \lambda^\pm(\omega, L)$ *is defined by*

$$\lambda^\pm = \frac{\alpha + \beta \pm \sqrt{(\alpha-\beta)^2 + 4\gamma\zeta}}{2},$$

with

$$\alpha = s_1 s_3 s_4 - s_2 s_4,\ \beta = -s_6 s_7 + s_5 s_6 s_8,\ \gamma = s_3 s_4 s_7 - s_4 s_8,\ \zeta = -s_1 s_6 + s_2 s_5 s_6.$$

This follows from the computation of the roots of the characteristic polynomial of M, which is biquadratic. The corresponding operators to (6) are non-local in time. In the next subsection, we therefore approximate the optimal operators by local ones.

2.2 Local Transmission Conditions

We approximate the optimal choice $\sigma_{k,\ell}$ in (6) by polynomials in ω :

$$\sigma_{1,2}^{\text{app}} = \frac{p_{1,2} + a_2}{2} + \frac{q_{1,2}}{2} i\omega, \quad \sigma_{2,1}^{\text{app}} = \frac{p_{2,1} - a_1}{2} + \frac{q_{2,1}}{2} i\omega,$$
$$\sigma_{2,3}^{\text{app}} = \frac{p_{2,3} + a_3}{2} + \frac{q_{2,3}}{2} i\omega, \quad \sigma_{3,2}^{\text{app}} = \frac{p_{3,2} - a_2}{2} + \frac{q_{3,2}}{2} i\omega.$$

In order to simplify the min-max problem, we will consider the following cases for the choice of $p_{k,\ell}$ and $q_{k,\ell}$:

1. (Robin) $p_{k,\ell} = p$, $q_{k,\ell} = 0$,
2. (Zeroth order) $p_{1,2} = p_{3,2} = p_1$, $p_{2,1} = p_{2,3} = p_2$, $q_{k,\ell} = 0$,
3. (First order) $p_{k,\ell} = p$, $q_{k,\ell} = q$,
4. (First order scaled) $p_{k,\ell} = p$, $q_{1,2} = \varphi_2 q$, $q_{2,1} = \varphi_1 q$, $q_{2,3} = \varphi_3 q$, $q_{3,2} = \varphi_2 q$.

Then, the parameters are chosen in order to minimize the convergence factor, i.e. we solve, for $\boldsymbol{p} = p$ in case 1, $\boldsymbol{p} = (p_1, p_2)$ in case 2, and $\boldsymbol{p} = (p, q)$ in cases 3 and 4, the min-max problem

$$\delta_m(L) = \min_{\boldsymbol{p}} \left(\max_{\omega_0 \le \omega \le \omega_{\max}} \rho(\omega, \boldsymbol{p}, \boldsymbol{\varphi}, \boldsymbol{a}, \boldsymbol{\nu}, b, L) \right), \tag{7}$$

where ρ is the spectral radius of M, in which we have replaced $\sigma_{k,\ell}$ by $\sigma_{k,\ell}^{\text{app}}$, and m is the order of the approximation. In numerical computations, the frequencies can be restricted to $\omega_{\max} = \frac{\pi}{\Delta t}$, where Δt is the time step, and $\omega_0 = \frac{\pi}{T}$.

UNCORRECTED PROOF

Theorem 1. *We suppose that $a_k = a$, $\varphi_k = \varphi$ and $\nu_k = \nu$, $1 \le k \le 3$, thus $d_k = d$ in* (4)*. Let us consider the Robin case ($\boldsymbol{p} = p$) and the first order case ($\boldsymbol{p} = (p,q)$). Then the convergence factor reduces to*

$$\rho(\omega,\boldsymbol{p},\varphi,a,\nu,b,L) = \sqrt{\left|\frac{\sigma-\sqrt{d}}{\sigma+\sqrt{d}}\right| \max\left(\left|\frac{\sigma-\mu}{\sigma+\mu}\right|,\left|\frac{\sigma-\eta}{\sigma+\eta}\right|\right)}$$

with

$$\mu = \sqrt{d}\left(\frac{1+e^{-\frac{\sqrt{d}}{2\nu}L}}{1-e^{-\frac{\sqrt{d}}{2\nu}L}}\right),\ \eta = \frac{\sqrt{d}}{\mu},$$

and with $\sigma = p$ in the Robin case, and $\sigma = p + qi\omega$ in the first order case. Let $L > 0$ given. Let $\delta_0(L)$ (resp. $\delta_1(L)$) be the solution of (7) *for the Robin case (resp. the first order case). For $m = 0$ and $m = 1$, we have $|\delta_m(L)| < 1$.*

3 Numerical Results

We use the DG-OSWR method in [4] based on a discontinuous Galerkin method in time, with $\mathbf{P}_1$ finite elements in space in each subdomain. We present an example inspired from nuclear waste simulations, with discontinuous coefficients, and different time and space steps in the subdomains $\Omega_2 = (0.4954, 0.5047)$ (repository), $\Omega_1 = (0, 0.4954)$ and $\Omega_3 = (0.5047, 1)$ (host rock). The parameters for the three subdomains are shown in Table 1. The final time is $T = 0.04$.

	φ	ν	a	b	Δx	Δt
$\Omega_1 \cup \Omega_3$	0.06	0.06	1	0	$5\,10^{-3}$	$T(5\,10^{-3})$
Ω_2	0.1	1	1	0	$5\,10^{-4}$	$T(1\,10^{-3})$

Table 1. Physical and numerical parameters

Let $\boldsymbol{p}_3^\star$ (resp. $\boldsymbol{p}_2^\star$) be the parameters derived from a numerical minimization of the three domains convergence factor in (7) (resp. from the two half-spaces convergence factor in [3]). Figure 1 shows $\rho(\omega,\boldsymbol{p}_3^\star,L)$ (solid line) and $\rho(\omega,\boldsymbol{p}_2^\star,L)$ (dashed line) versus ω for $\Delta t = T(5\ 10^{-3})$. We observe that the solution of (7) is characterized by an equioscillation property (at the star marks), as in the two half-spaces case (see [2]). Moreover, for first order transmission conditions, we see that a scaling with the porosity is important only when the parameters are computed from the two half-spaces analysis.

On Fig. 2 we show the error after 20 iterations when running the algorithm on the discretized problem, with $u_0 = f = 0$ and random initial guess on the interfaces, for various values of the Robin parameter p (left) and the zeroth order parameters p_1, p_2 (right) (in that case, the values obtain with the two half-spaces analysis is not in the range values of the figure).

UNCORRECTED PROOF

this figure will be printed in b/w

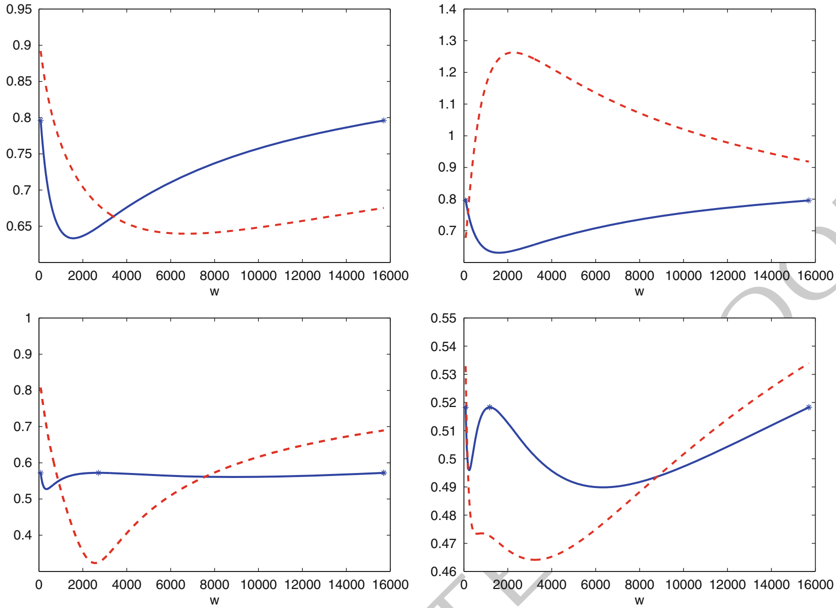

Fig. 1. Convergence factor $\rho(\omega, \boldsymbol{p}_3^*, L)$ (*solid line*) and $\rho(\omega, \boldsymbol{p}_2^*, L)$ (*dashed line*) versus ω: *Top left*: Robin, *top right*: zeroth order, *left bottom*: first order, *right bottom*: first order scaled

this figure will be printed in b/w

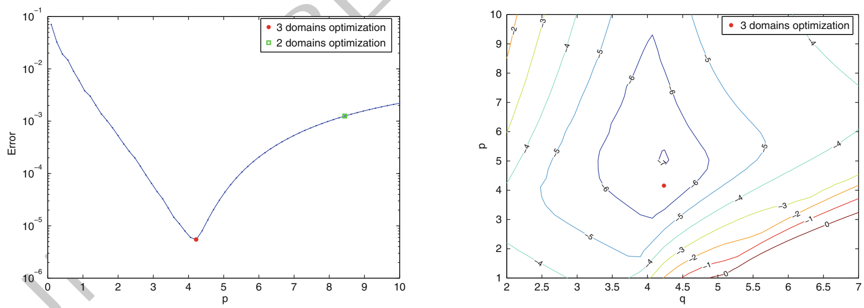

Fig. 2. Error after 20 iterations: *Left*: for various values of the Robin parameter p (the *lower left star marks* $p_3^\star$ whereas the *upper right circle* shows $p_2^\star$), *Right*: the level curves for various values of the zeroth order parameters p_1, p_2 (the *star marks* the parameter $\boldsymbol{p}_3^\star$)

UNCORRECTED PROOF

this figure will be printed in b/w

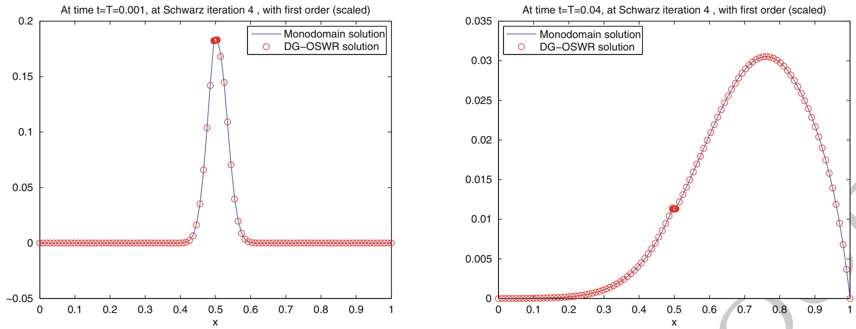

Fig. 3. Evolution of the monodomain solution (*solid line*) and the OSWR solution at iteration 4 (*circle line*): at $t = 0.001$ (*left*), $t = T = 0.04$ (*right*)

this figure will be printed in b/w

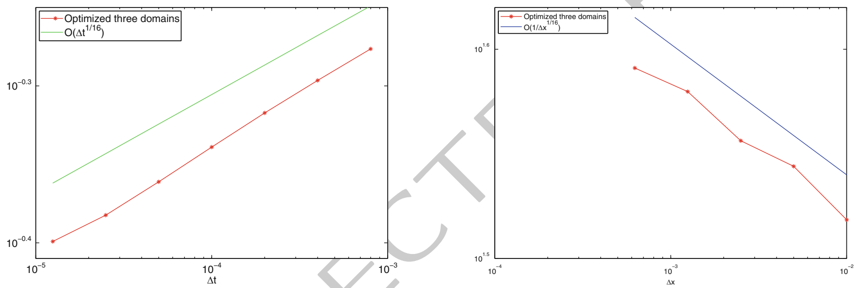

Fig. 4. Asymptotic behavior as the mesh is refined: on the *left* $R(\Delta t)$ and on the *right* where $\Delta t = O(\Delta x)$, the rate for the optimized Schwarz waveform relaxation algorithm with optimized first order (scaled) transmission conditions

UNCORRECTED PROOF

On Fig. 3, the solution, with first order (scaled) conditions, at iteration 4 is shown for an initial condition equal to 1 in Ω_2 and 0 elsewhere.

AQ1 Figure 4 shows on the left $R(\Delta t) = 1 - \max_{\pi/T \le \omega \le \pi/\Delta t} \rho(\omega, \boldsymbol{p}_3^\star, L))$ versus Δt, i.e. the convergence factor behaves like $1 - O(\Delta t)^{1/16}$, with first order (scaled) optimized transmission conditions. On the right, we run the OSWR algorithm until the error becomes smaller than 10^{-11}, and count the number of iterations. We start with $\Delta t = T/100$ in each subdomain, and repeat this experiment dividing Δx and Δt by 2 several times. We observe that the asymptotic result on the left predicts very well the numerical behavior of the algorithm given on the right.

Bibliography

[1] Stephan Schumacher Alain Bourgeat, Michel Kern and Jean Talandier. The couplex test cases: Nuclear waste disposal simulation. *Computational Geosciences*, 8:83–98, 2004.

[2] D. Bennequin, M.J. Gander, and L.Halpern. A homographic best approximation problem with application to optimized Schwarz waveform relaxation. *Math. Comp.*, 78:185–223, 2009.

[3] M.J. Gander, L. Halpern, and M. Kern. Schwarz waveform relaxation method for advection–diffusion–reaction problems with discontinuous coefficients and non-matching grids. In O.B. Widlund and D.E. Keyes, editors, *Decomposition Methods in Science and Engineering XVI*, volume 55 of *Lecture Notes in Computational Science and Engineering*, pages 916–920. Springer, 2007.

[4] L. Halpern, C. Japhet, and J. Szeftel. Discontinuous Galerkin and nonconforming in time optimized Schwarz waveform relaxation. In O. Widlund Y. Huang, R. Kornhuber and J. Xu, editors, *Domain Decomposition Methods in Science and Engineering XIX*, volume 78 of *Lecture Notes in Computational Science and Engineering*, pages 133–140, 2010.

[5] L. Halpern, C. Japhet, and P. Omnes. Nonconforming in time domain decomposition method for porous media applications. In J. C. F. Pereira and A. Sequeira, editors, *V European Conference on Computational Fluid Dynamics ECCOMAS CFD*, Lisbon, Portugal,14–17 June 2010.

[6] V. Martin. An optimized Schwarz waveform relaxation method for the unsteady convection diffusion equation in two dimensions. *Appl. Numer. Math.*, 52:401–428, 2005.

[7] Alfio Quarteroni and Alberto Valli. *Domain Decomposition Methods for Partial Differential Equations*. Oxford Science Publications, 1997.

UNCORRECTED PROOF